AIAA SciTech Forum
January 3-7, 2022, San Diego, CA & Virtual
AIAA SCITECH 2022 Forum

10.2514/6.2022-1599

Structure Identification Method for Nonsmooth and Singular Optimal Control Problems

Elisha R. Pager*
Anil V. Rao†

University of Florida
Gainesville, FL 32611

Abstract

This work introduces a method developed for identifying the structure of nonsmooth and singular optimal control problems using jump function approximations and the Hamiltonian of the system. The structure identification procedure is paired with a regularization method to solve the problem using a multiple-domain Legendre-Gauss-Radau (LGR) collocation. The method is divided into several parts. First, the structure detection method described identifies switch times in the control and analyzes the corresponding switching function for segments where the solution is either bang-bang or singular. Second, after the structure has been detected, the domain is decomposed into multiple domains such that the multiple-domain formulation includes additional decision variables that represent the switch times in the optimal control. In domains classified as bang-bang, the control is set to either its upper or lower limit. In domains identified as singular, a regularization procedure is employed. The method is demonstrated on an example with a finite and infinite-order singular arc. The results demonstrate that the method of this paper can accurately identify the control structure of a complex optimal control problem. Furthermore, when the structure identification method is paired with a strategy for solving singular optimal control problems accurate solutions are obtained. The results are compared against a previously developed mesh refinement method that is not tailored for solving nonsmooth and/or singular optimal control problems.

1 Nomenclature

$\mathbf{a}$	=	right-hand side of dynamics
$\mathbf{b}$	=	boundary conditions
d	=	domain index
$\mathbf{g}, \mathbf{h}$	=	dynamics components that are not a function of the control
$\mathbf{D}$	=	Legendre-Gauss-Radau differentiation matrix
D	=	total number of domains used in a phase
$\mathbf{f}$	=	Hamiltonian component that is not a function of the control
$\mathcal{H}$	=	Hamiltonian of optimal control problem
i	=	collocation point row index
j	=	collocation point column index
$\mathcal{J}$	=	objective functional
k	=	mesh index
K	=	number of mesh intervals in a domain
$\mathcal{K}$	=	total number of singular domains
$\ell_j^{(k)}$	=	Lagrange polynomial j of mesh interval k
$\mathcal{L}$	=	integrand appearing in Lagrange cost

*Ph.D. Candidate, Department of Mechanical and Aerospace Engineering, University of Florida, Gainesville, Florida 32611-6250. Email: epager@ufl.edu.

†Professor, Department of Mechanical and Aerospace Engineering, University of Florida, Gainesville, FL 32611-6250. E-mail: anilvrao@ufl.edu. Corresponding Author.

$\mathcal{M}$ = Mayer cost
n_u = number of controls
n_x = number of states
N = total number of collocation points
$\mathcal{P}_d$ = time domain d
$\mathcal{I}_k$ = mesh interval k
t = time on $[t_0, t_f]$
$\mathbf{u}$ = control in time horizon
$\mathbf{U}$ = matrix of control characterization at LGR collocation points
$\mathcal{U}$ = admissible control set
$\mathbf{w}$ = LGR weights
$\mathbf{x}$ = state in time horizon
$\mathbf{X}$ = matrix of state approximation at discretized LGR points
α = approximating function of the control
$\boldsymbol{\lambda}$ = costates at LGR collocation points
ϕ = switching function
τ = time on $[-1, +1]$

2 Introduction

Optimal control problems arise in many engineering applications due to the need to optimize the performance of a controlled dynamical system. In general, optimal control problems do not have analytic solutions and must be solved numerically. A key challenge in solving an optimal control problem numerically arises due to the fact that most optimal control problems are subject to constraints on the system that often take the form of limits imposed on functions of either the control and/or the state. As a result, constrained optimal control problems often have nonsmooth solutions, where the nonsmoothness arises in the form of instantaneous switches in the control. Moreover, many control constrained optimal control problems have solutions that lie on one or more singular arcs. The existence of a singular arc makes solving constrained optimal control problems even more challenging because Pontryagin's minimum principle (that is, the first and second-order optimality conditions) fail to yield a complete solution along the singular arc. As a result, when applying a computational method to a problem whose solution lies on a singular arc, standard methods produce nonsensical results. Before tackling the challenge of determining the optimal control along a singular arc, the ability to detect the presence of singular arc must first be addressed. This research is motivated by the importance of solving singular optimal control problems by focusing on identifying singular arcs in the control solution.

Computational issues arise when a solution to an optimal control problem is either nonsmooth or singular. The difficulty with such optimal control problems is twofold. First, the precise locations of any discontinuities and the structure of the control must be identified. More recently, the idea of using variable mesh refinement methods and structure detection methods has been developed [1, 2, 3, 4, 5]. Unlike static mesh refinement methods such as those found in Refs. [6, 7, 8], variable mesh refinement methods work by including parameters in the optimization that define the location of the discontinuities. The methods in Refs. [1, 2, 3] use the Lagrange multipliers to detect the switch point locations in the control structure and then place variable mesh points to represent the switch times in the NLP, while Refs. [4, 5] use the switching function and a sensitivity analysis to place moving finite elements at the switch point locations. Furthermore, Ref. [9] describes a mesh refinement method for solving bang-bang optimal control problems based on the switching function associated with the Hamiltonian. More recently, in Ref. [10] a switch point algorithm was developed for optimizing over the locations of switch points in a nonsmooth control solution, but a priori knowledge of the switch points existence is required. Finally, methods that utilize structure detection on a static mesh are described in Refs. [11, 12].

The second difficulty in solving optimal control problems with nonsmooth or singular solutions arises when the optimal control is singular. Several approaches have been developed for solving singular optimal control problems using both indirect and direct methods. A majority of these methods typically employ either a regularization approach or use of the optimality conditions with an indirect method to solve for the singular control (see Refs. [13, 14]). A regularization method transforms the singular control problem into a series of nonsingular problems by minimizing the sum of the original objective and a regularization

term, where the regularization term is often a quadratic function of the control. The identification procedure described in this paper is paired with a regularization method introduced in Refs [15, 16] to obtain a complete solution to the singular or nonsmooth optimal control problem.

Numerical methods for optimal control typically fall into two broad categories: indirect methods and direct methods. In an indirect method, the first-order variational optimality conditions are derived, and the optimal control problem is converted to a Hamiltonian boundary-value problem (HBVP). In a direct method, the state and/or the control are approximated, and the optimal control problem is transcribed into a finite-dimensional nonlinear programming problem (NLP) [17]. The NLP is then solved numerically using well-developed software such as *SNOPT* [18] or *IPOPT* [19]. The structure identification method developed in this paper is formulated to work with a direct method. More specifically, a direct Gaussian quadrature orthogonal collocation method is used [20, 21, 22, 23] where the state is approximated using a basis of Lagrange polynomials and the support points of the polynomials are chosen to be the points associated with a Gaussian quadrature. In particular, the collocation is performed at the Legendre-Gauss-Radau (LGR) points [6, 21, 22, 23, 24]. A new multiple-domain formulation of the well-established LGR collocation method is adopted from Ref. [16] where the structure identified by the method of this paper can be implemented as domains and domain interface variables in the NLP formulation.

The main contributions of this work is the development of a structure identification method that pairs with a regularization method to identify and solve nonsmooth and/or singular optimal control problems. The method of this paper exploits the advantages of using a multiple-domain reformulation of LGR collocation with a regularization procedure to accurately detect and solve a singular optimal control problem. Identification of control switch times using jump function approximations [25] combined with identification of bang-bang and singular arcs is used to analyze the structure of a coarse control solution. The multiple-domain LGR collocation is used to partition the time horizon into domains with additional decision variables assigned at the identified switch time locations. Finally, the newly partitioned problem structure is paired with the regularization method developed in Refs. [15, 16] to obtain a highly accurate solution to the problem.

It is noted that Ref. [16] provides a comprehensive method for solving optimal control problems whose solutions contain bang-bang or singular arcs in the optimal control. The method described in Ref. [16] not only automatically detects the structure of a nonsmooth optimal control solution, including the identification of singular arcs, but also performs a decomposition of the optimal control problem into multiple domains and introduces variables into the problem that identify the endpoints of each newly introduced domain. In addition, the method of Ref. [16] includes a regularization method for determining a singular control. Because this paper focuses on structure identification, the work described here is only a portion of the more comprehensive method developed by the authors in Ref. [16].

The remainder of the paper is organized as follows. Section 3 introduces the Bolza optimal control problem and a brief overview of nonsmooth optimal control. Section 4 describes the multiple-domain Legendre-Gauss-Radau collocation used to transcribe the multiple-domain Bolza optimal control problem. Section 5 describes the structure identification method for detecting bang-bang and singular arcs in an optimal control problem. Section 6 demonstrates the method on a complex aerospace example. Finally, Section 7 provides conclusions on this research.

3 Optimal Control Problem

Without loss of generality, consider the following single-phase optimal control problem in Bolza form defined on the time horizon $t \in [t_0, t_f]$. Determine the state $\mathbf{x}(t) \in \mathbb{R}^{n_x}$, the control $\mathbf{u}(t) \in \mathbb{R}^{n_u}$, and the terminal time $t_f \in \mathbb{R}$ that minimize the objective functional

$$\mathcal{J} = \mathcal{M}(\mathbf{x}(t_0), t_0, \mathbf{x}(t_f), t_f) + \int_{t_0}^{t_f} \mathcal{L}(\mathbf{x}(t), \mathbf{u}(t), t)\ dt\ , \tag{1}$$

subject to the dynamic constraints

$$\frac{d\mathbf{x}(t)}{dt} \equiv \dot{\mathbf{x}}(t) = \mathbf{a}(\mathbf{x}(t), \mathbf{u}(t), t)\ , \tag{2}$$

the control constraints

$$\mathbf{u}_{\min} \leq \mathbf{u}(t) \leq \mathbf{u}_{\max}\ , \tag{3}$$

and the boundary conditions

$$\mathbf{b}_{\min} \leq \mathbf{b}(\mathbf{x}(t_0), t_0, \mathbf{x}(t_f), t_f) \leq \mathbf{b}_{\max} \ . \tag{4}$$

The Bolza optimal control problem given in Eqs. (1)–(4) gives rise to the following first-order calculus of variations [26, 27] conditions:

$$\dot{\mathbf{x}}(t) = \left[\frac{\partial \mathcal{H}}{\partial \boldsymbol{\lambda}}\right]^{\mathsf{T}} = \mathcal{H}_{\boldsymbol{\lambda}}^{\mathsf{T}}, \tag{5}$$

$$\dot{\boldsymbol{\lambda}}(t) = -\left[\frac{\partial \mathcal{H}}{\partial \mathbf{x}}\right]^{\mathsf{T}} = -\mathcal{H}_{\mathbf{x}}^{\mathsf{T}}, \tag{6}$$

$$\mathbf{0} = \frac{\partial \mathcal{H}}{\partial \mathbf{u}} = \mathcal{H}_{\mathbf{u}}, \tag{7}$$

where $\boldsymbol{\lambda}(t) \in \mathbb{R}^{n_x}$ is the costate,

$$\mathcal{H}(\mathbf{x}(t), \mathbf{u}(t), \boldsymbol{\lambda}(t), \boldsymbol{\mu}(t), t) = \mathcal{L}(\mathbf{x}(t), \mathbf{u}(t), t) + \boldsymbol{\lambda}^{\mathsf{T}}(t)\mathbf{a}(\mathbf{x}(t), \mathbf{u}(t), t), \tag{8}$$

is the augmented Hamiltonian, and $\mathcal{U}$ is the admissible control set. Finally, the transversality conditions are given by

$$\boldsymbol{\lambda}(t_0) = -\frac{\partial \mathcal{M}}{\partial \mathbf{x}(t_0)} + \boldsymbol{\nu}^{\mathsf{T}} \frac{\partial \mathbf{b}}{\partial \mathbf{x}(t_0)} \quad , \quad \boldsymbol{\lambda}(t_f) = \frac{\partial \mathcal{M}}{\partial \mathbf{x}(t_f)} - \boldsymbol{\nu}^{\mathsf{T}} \frac{\partial \mathbf{b}}{\partial \mathbf{x}(t_f)} \tag{9}$$

$$\mathcal{H}(t_0) = \frac{\partial \mathcal{M}}{\partial t_0} - \boldsymbol{\nu}^{\mathsf{T}} \frac{\partial \mathbf{b}}{\partial t_0} \quad , \quad \mathcal{H}(t_f) = -\frac{\partial \mathcal{M}}{\partial t_f} + \boldsymbol{\nu}^{\mathsf{T}} \frac{\partial \mathbf{b}}{\partial t_f} \tag{10}$$

where $\boldsymbol{\nu}$ is the Lagrange multiplier associated with the boundary conditions. Equations (5) and (6) form what is classically known as a *Hamiltonian system* [26]. The conditions in Eqs. (9) and (10) are called *transversality conditions* [26, 27] on the boundary values of the costate. For some problems, the control cannot be uniquely determined, either implicitly or explicitly, from the optimality conditions given in Eqs. (5)–(10). In such cases, the weak form of Pontryagin's minimum principle can be used which solves for the permissible control that minimizes the Hamiltonian in Eq. (8). If $\mathcal{U}$ is the set of permissible controls, then Pontryagin's minimum principle states that the optimal control, $\mathbf{u}(t)$, satisfies the condition

$$\mathcal{H}(\mathbf{x}^*(t), \mathbf{u}^*(t), \boldsymbol{\lambda}^*(t), t) \leq \mathcal{H}(\mathbf{x}^*(t), \mathbf{u}, \boldsymbol{\lambda}^*(t), t), \quad \mathbf{u} \in \mathcal{U}. \tag{11}$$

The Hamiltonian system, together with the original boundary conditions, and the costate transversality conditions, forms a *Hamiltonian boundary-value problem* (HBVP) [26, 27]. Any solution $(\mathbf{x}^*(t), \mathbf{u}^*(t), \boldsymbol{\lambda}^*(t), \boldsymbol{\nu}^*)$ to the HBVP is called an *extremal* solution.

A singular arc will occur in a solution when the application of Pontryagin's minimum principle fails to yield a complete solution of the optimal control [27]. This phenomena can occur in many situations but is most common when the dynamics are linear in the control and the control is bounded, or the Hamiltonian is not an explicit function of time. It should be noted that singular arcs can also occur in other situations, but in order to provide structure to the method developed in this paper, only problems that fall into the aforementioned categories will be considered.

For simplicity, it is assumed that the control is scalar, $u(t) \in \mathbb{R}$, but the following discussion can be extended to multiple control components as shown in the example provided in Section 6. Suppose the optimal control problem described in Eqs. (1)–(4) is nonsmooth and singular as defined by the assumptions mentioned previously. The dynamics can now be rewritten in the affine form as

$$\dot{\mathbf{x}}(t) = \mathbf{a}(\mathbf{x}(t), u(t)) = \mathbf{g}(\mathbf{x}(t)) + \mathbf{h}(\mathbf{x}(t))u(t), \tag{12}$$

where $\mathbf{g}(\mathbf{x}(t))$ and $\mathbf{h}(\mathbf{x}(t))$ are not functions of the control. The Hamiltonian from Eq. (8) is redefined as

$$\mathcal{H}(\mathbf{x}(t), \boldsymbol{\lambda}(t), \boldsymbol{\mu}(t), u(t), t) = \mathbf{f}(\mathbf{x}(t), \boldsymbol{\lambda}(t)) + \phi^{\mathsf{T}}(\mathbf{x}(\mathbf{t}), \boldsymbol{\lambda}(t))u(t), \tag{13}$$

where $\mathbf{f}(\mathbf{x}(t), \boldsymbol{\lambda}(t))$ and $\phi(\mathbf{x}(t), \boldsymbol{\lambda}(t))$ are the components of the Hamiltonian that are not a function of the control, and mixed state and control path constraints are not considered. The strong form of Pontryagin's Minimum Principle (PMP), Eq. (11), is applied as follows

$$\frac{\partial \mathcal{H}}{\partial u} = \mathcal{H}_u = \phi(\mathbf{x}(t), \boldsymbol{\lambda}(t)) = 0. \tag{14}$$

Note that the control does not appear in Eq. (14) because the Hamiltonian is linear in the control. A singular arc is characterized as $\mathcal{H}_u = 0$ and $\mathcal{H}_{uu}$ is singular everywhere on the arc. It is noted that $\mathcal{H}_{uu}$ is defined as follows

$$\mathcal{H}_{uu} = \frac{\partial}{\partial u}\mathcal{H}_u = \frac{\partial^2 \mathcal{H}}{\partial u \partial u}. \tag{15}$$

When this occurs, the reduced Hessian matrix associated with the corresponding NLP that arises from the direct transcription method of Section 4 is ill-conditioned such that the projected Hessian matrix is not positive definite. This leads to poor conditioning in the control profiles which often presents itself in the form of oscillations, or chattering behavior, in the control solution.

The sign and value of $\phi(\mathbf{x}(t), \boldsymbol{\lambda}(t))$ (where ϕ is called the switching function) determines if the control is called a *bang-bang* control or a *singular* control. The weak form of PMP [27] is used in the case of nonsmooth control and the minimization of the Hamiltonian leads to the following piecewise-continuous control, $u(t)$, that is dependent on the switching function as follows

$$u^*(t) = \underset{u(t)\in\mathcal{U}}{\arg\min}\,\mathcal{H} = \begin{cases} u_{\min} & , \quad \phi(\mathbf{x}(t), \boldsymbol{\lambda}(t)) > 0, \\ u_{\text{singular}} & , \quad \phi(\mathbf{x}(t), \boldsymbol{\lambda}(t)) = 0, \\ u_{\max} & , \quad \phi(\mathbf{x}(t), \boldsymbol{\lambda}(t)) < 0, \end{cases} \tag{16}$$

where the sign of the switching function, $\phi(\mathbf{x}(t), \boldsymbol{\lambda}(t))$, is determined by the state and the costate, and $\mathcal{U} \in [u_{\min}, u_{\max}]$ is the admissible control set. As the switching function $\phi(\mathbf{x}(t), \boldsymbol{\lambda}(t))$ changes sign, the control coincides with the sign changes by switching between its maximum and minimum values. Any time interval over which $\phi(\mathbf{x}(t), \boldsymbol{\lambda}(t))$ is zero is referred to as a singular arc and any control in the admissible control set will minimize the Hamiltonian. Furthermore, switching between nonsingular and singular arcs give rise to discontinuities on the state and control profiles, and the location of these transition points are referred to as *switch times*.

A common approach to determine unique singular controls over an arc is to repeatedly differentiate $\mathcal{H}_u$ with respect to time until the control explicitly appears

$$\frac{d^{(r)}}{dt^{(r)}}\mathcal{H}_u = 0, \quad (r = 0, 1, 2, \ldots). \tag{17}$$

An additional necessary condition for optimality is introduced to guarantee that the resulting singular control law is optimal. This condition is also referred to as the generalized Legendre-Clebsch condition [27, 28, 29],

$$(-1)^k \frac{\partial}{\partial u}\left[\frac{d^{2k}}{dt^{2k}}\mathcal{H}_u\right] \geq 0, \quad (k = 0, 1, 2, \ldots), \tag{18}$$

where k represents the order of the singular arc. While in some problems of interest it is possible to use Eq. (17) to determine a condition for the singular control, in many cases it is unable to produce the singular control (for example, if the order of the singular arc is infinite). Even in cases where the singular control could be determined from Eq. (17), taking derivatives higher than second-order is not easy to implement numerically or algorithmically.

4 Multiple-Domain Legendre-Gauss-Radau Collocation

In this paper, the previously developed *hp*–adaptive Legendre-Gauss-Radau (LGR) collocation method [6, 21, 22, 23, 24] is used to approximate the optimal control problem. Specifically, a multiple-domain reformulation of LGR collocation developed in Ref. [16] is briefly described in the remainder of this section. The multiple-domain formulation of LGR collocation divides the domain $t \in [t_0, t_f]$ into distinct partitions such that the endpoints of each partition are decision variables. The division into domains is obtained using a structure decomposition method as described in Section 5.3. The continuous-time Bolza optimal control problem described in Eqs. (1)–(4) is discretized using collocation at the Legendre-Gauss-Radau (LGR) points [21, 22, 23, 24]. The time horizon $t \in [t_0, t_f]$ may be divided into D time domains, $\mathcal{P}_d = [t_s^{[d-1]}, t_s^{[d]}] \subseteq [t_0, t_f]$, $d \in \{1, \ldots, D\}$, such that

$$\bigcup_{d=1}^{D} \mathcal{P}_d = [t_0, t_f] \ , \quad \bigcap_{d=1}^{D} \mathcal{P}_d = \{t_s^{[1]}, \ldots, t_s^{[D-1]}\} \ , \tag{19}$$

where $t_s^{[d]},\ d\in\{1,\ldots,D-1\}$ are the domain interface variables of the problem, $t_s^{[0]}=t_0$, and $t_s^{[D]}=t_f$. Thus, in the case where $D=1$ the phase consists of only a single domain $\mathcal{P}_1=[t_0,t_f]$ and $\{t_s^{[1]},\ldots,t_s^{[D-1]}\}=\emptyset$.

$$\begin{aligned} t &= \frac{t_s^{[d]}-t_s^{[d-1]}}{2}\tau+\frac{t_s^{[d]}+t_s^{[d-1]}}{2}\ , \\ \tau &= 2\frac{t-t_s^{[d-1]}}{t_s^{[d]}-t_s^{[d-1]}}-1\ . \end{aligned} \tag{20}$$

The interval $\tau\in[-1,+1]$ for each domain $\mathcal{P}_d$ is then divided into K mesh intervals, $\mathcal{I}_k=[T_{k-1},T_k]\subseteq[-1,+1],\ k\in\{1,\ldots,K\}$ such that

$$\bigcup_{k=1}^{K}\mathcal{I}_k=[-1,+1]\ ,\quad \bigcap_{k=1}^{K}\mathcal{I}_k=\{T_1,\ldots,T_{K-1}\}\ , \tag{21}$$

and $-1=T_0<T_1<\ldots<T_{K-1}<T_K=+1$. For each mesh interval, the LGR points used for collocation are defined in the domain of $[T_{k-1},T_k]$ for $k\in\{1,\ldots,K\}$. The state of the continuous optimal control problem is then approximated in mesh interval $\mathcal{I}_k,\ k\in\{1,\ldots,K\}$, as

$$\mathbf{x}^{(k)}(\tau)\approx\mathbf{X}^{(k)}(\tau)=\sum_{j=1}^{N_k+1}\mathbf{X}_j^{(k)}\ell_j^{(k)}(\tau)\ ,\quad \ell_j^{(k)}(\tau)=\prod_{\substack{l=1\\ l\neq j}}^{N_k+1}\frac{\tau-\tau_l^{(k)}}{\tau_j^{(k)}-\tau_l^{(k)}}\ , \tag{22}$$

where $\ell_j^{(k)}(\tau)$ for $j\in\{1,\ldots,N_k+1\}$ is a basis of Lagrange polynomials on $\mathcal{I}_k$, $\left(\tau_1^{(k)},\ldots,\tau_{N_k}^{(k)}\right)$ are the set of N_k Legendre-Gauss-Radau (LGR) collocation points in the interval $[T_{k-1},T_k)$, $\tau_{N_k+1}^{(k)}=T_k$ is a non-collocated support point, and $\mathbf{X}_j^{(k)}\equiv\mathbf{X}^{(k)}(\tau_j^{(k)})$. Differentiating $\mathbf{X}^{(k)}(\tau)$ in Eq. (22) with respect to τ gives

$$\frac{d\mathbf{X}^{(k)}(\tau)}{d\tau}=\sum_{j=1}^{N_k+1}\mathbf{X}_j^{(k)}\frac{d\ell_j^{(k)}(\tau)}{d\tau}\ . \tag{23}$$

The dynamics are then approximated at the N_k LGR points in mesh interval $k\in\{1,\ldots,K\}$ as

$$\sum_{j=1}^{N_k+1}D_{lj}^{(k)}\mathbf{X}_j^{(k)}-\frac{t_f-t_0}{2}\mathbf{a}\left(\mathbf{X}_l^{(k)},\mathbf{U}_l^{(k)},t(\tau_l^{(k)},t_0,t_f)\right)=\mathbf{0}\ ,\quad l\in\{1,\ldots,N_k\}\ , \tag{24}$$

where

$$D_{lj}^{(k)}=\frac{d\ell_j^{(k)}(\tau_l^{(k)})}{d\tau}\ ,\quad l\in\{1,\ldots,N_k\}\ ,\ j\in\{1,\ldots,N_k+1\}\ ,$$

are the elements of the $N_k\times(N_k+1)$ *Legendre-Gauss-Radau differentiation matrix* in mesh interval $\mathcal{I}_k$, $k\in\{1,\ldots,K\}$, and $\mathbf{U}_l^{(k)}$ is the approximation of the control at the l^{th} collocation point in mesh interval $\mathcal{I}_k$. The time variables t_0 and t_f in Eq. (24) represent the initial and final domain interface variables, $t_s^{[d-1]}$ and $t_s^{[d]}$, on the domain $\mathcal{P}_d$. It is noted that continuity in the state and time between mesh intervals $\mathcal{I}_{k-1}$ and $\mathcal{I}_k$, $k\in\{1,\ldots,K\}$, is enforced by using the same variables to represent $\mathbf{X}_{N_{k-1}+1}^{(k-1)}$ and $\mathbf{X}_1^{(k)}$, while continuity in the state between the domains $\mathcal{P}_{d-1}$ and $\mathcal{P}_d$, $d\in\{2,\ldots,D\}$, is achieved by using the same variables to represent $\mathbf{X}_{N^{[d-1]}+1}^{[d-1]}$ and $\mathbf{X}_1^{[d]}$ where the superscript $[d]$ is used to denote the d^{th} time domain, $\mathbf{X}_j^{[d]}$ denotes the value of the state approximation at the j^{th} discretization point in the time domain $\mathcal{P}_d$, and $N^{[d]}$ is the total number of collocation points used in time domain $\mathcal{P}_d$ computed by

$$N^{[d]}=\sum_{k=1}^{K^{[d]}}N_k^{[d]}\ . \tag{25}$$

The Legendre-Gauss-Radau approximation of the multiple-domain optimal control problem results in the following nonlinear programming problem (NLP). Minimize the objective function

$$\mathcal{J}=\mathcal{M}(\mathbf{X}_1^{[1]},t_0,\mathbf{X}_{N^{[D]}+1}^{[D]},t_f)+\sum_{d=1}^{D}\frac{t_s^{[d]}-t_s^{[d-1]}}{2}\left[\mathbf{w}^{[d]}\right]^{\mathsf{T}}\mathbf{L}^{[d]}\ , \tag{26}$$

subject to the collocated dynamic constraints

$$\boldsymbol{\Delta}^{[d]} = \mathbf{D}^{[d]}\mathbf{X}^{[d]} - \frac{t_s^{[d]} - t_s^{[d-1]}}{2}\mathbf{A}^{[d]} = \mathbf{0} \ , \quad d \in \{1, \ldots, D\} \ , \tag{27}$$

the path constraints

$$\mathbf{c}_{\min} \leq \mathbf{C}_j^{[d]} \leq \mathbf{c}_{\max} \ , \quad j \in \{1, \ldots, N^{[d]}\} \ , \ d \in \{1, \ldots, D\} \ , \tag{28}$$

the control constraints

$$\mathbf{u}_{\min} \leq \mathbf{U}_j^{[d]} \leq \mathbf{u}_{\max} \ , \quad j \in \{1, \ldots, N^{[d]}\} \ , \ d \in \{1, \ldots, D\} \ , \tag{29}$$

the boundary conditions

$$\mathbf{b}_{\min} \leq \mathbf{b}(\mathbf{X}_1^{[1]}, t_0, \mathbf{X}_{N^{[D]}+1}^{[D]}, t_f) \leq \mathbf{b}_{\max} \ . \tag{30}$$

and the continuity constraints

$$\mathbf{X}_{N^{[d-1]}+1}^{[d-1]} = \mathbf{X}_1^{[d]} \ , \ d \in \{2, \ldots, D\} \ , \tag{31}$$

noting that Eq. (31) is implicitly satisfied by employing the same variable in the NLP for $\mathbf{X}_{N^{[d-1]}+1}^{[d-1]}$ and $\mathbf{X}_1^{[d]}$.

Estimates of the costate may be obtained at each of the discretization points in the time domain $\mathcal{P}_d, d \in \{1, \ldots, D\}$ using the transformation [21, 22, 23],

$$\begin{aligned} \boldsymbol{\lambda}^{[d]} &= (\mathbf{W}^{[d]})^{-1}\boldsymbol{\Lambda}^{[d]} \ , \\ \boldsymbol{\lambda}_{N^{[d]}+1}^{[d]} &= (\mathbf{D}_{N^{[d]}+1}^{[d]})^{\mathsf{T}}\boldsymbol{\Lambda}^{[d]} \ , \end{aligned} \tag{32}$$

where $\boldsymbol{\lambda}^{[d]} \in \mathbb{R}^{N^{[d]} \times n_x}$ is a matrix of the costate estimates at the collocation points in time domain $\mathcal{P}_d$, $\mathbf{W}^{[d]} = \text{diag}(\mathbf{w}^{[d]})$ is a diagonal matrix of the LGR weights at the collocation points in time domain $\mathcal{P}_d$, $\boldsymbol{\Lambda}^{[d]} \in \mathbb{R}^{N^{[d]} \times n_x}$ is a matrix of the NLP multipliers obtained from the NLP solver corresponding to the defect constraints at the collocation points in time domain $\mathcal{P}_d$, $\boldsymbol{\lambda}_{N^{[d]}+1}^{[d]} \in \mathbb{R}^{1 \times n_x}$ is a row vector of the costate estimates at the non-collocated end point in time domain $\mathcal{P}_d$, and $\mathbf{D}_{N^{[d]}+1}^{[d]} \in \mathbb{R}^{N^{[d]} \times 1}$ is the last column of the LGR differentiation matrix in time domain $\mathcal{P}_d$.

The aforementioned multiple-domain LGR formulation is summarized as follows. First, a single *phase* problem on $t \in [t_0, t_f]$ is divided into D *domains*, $\mathcal{P}_d = [t_s^{[d-1]}, t_s^{[d]}]$, $d \in \{1, \ldots, D\}$. Each of the D domains are then mapped to the interval $\tau^{[d]} \in [-1, +1]$, $d \in \{1, \ldots, D\}$. The interval $\tau^{[d]} \in [-1, +1]$, $d \in \{1, \ldots, D\}$ for each domain is then divided into K *mesh intervals*, $\mathcal{I}_k = [T_{k-1}, T_k] \subseteq [-1, +1]$, $k \in \{1, \ldots, K\}$. Finally, the intersection of each domain is determined by the *domain interface variables*, $t_s^{[d]}$, $d \in \{1, \ldots, D-1\}$.

5 Structure Identification Method

In this section, a brief overview of the structure identification method used in solving bang-bang and singular optimal control problems is provided, see Ref. [16] for more details. The method consists of two stages. The first stage of the method described in the following sections details the identification of the control structure and the decomposition of the optimal control problem into a multiple-domain optimal control problem dictated by the discontinuities identified that are represented as domain interface variables. These domain interface variables are then treated as additional decision variables in the nonlinear programming problem (NLP). The first stage is only implemented on the first mesh iteration. The second stage adds additional constraints and iterative procedures to the NLP depending on the structure identification's classification of a domain as being bang-bang or singular in order to constrain the modified optimal control problem correctly. Details on the constraints and methods applied in each type of domain can be found in Refs.[15] and [16].

Assume now that the optimal control problem formulated in Section 3 under the assumptions of Section 3 has been transcribed into a NLP using multiple-domain LGR collocation developed in Section 4 with $D = 1$ (that is, a single domain is used). The solution obtained from the NLP then leads to estimates of the state, the control, and the costate. Assume further that the mesh refinement accuracy tolerance is not satisfied. As a result, mesh refinement is required which simultaneously enables the decomposition of the problem into domains that are either bang-bang, singular, or regular. This decomposition is obtained using structure identification as described now.

5.1 Identification of Control Switch Times

Discontinuities in each component of the control are identified using jump function approximations of the control solution as shown in Ref. [25]. In particular, the method given in Ref. [25] is employed here because it is effective for estimating locations of nonsmoothness in the optimal control. The process of using jump function approximations is beyond the scope of this paper and the author refers the reader to Ref. [16] for further details on using jump function approximations to identify discontinuities.

The identified discontinuities obtained from the jump function approximations are referred to as b_i, $i = \{1, \ldots, n_d\}$ where n_d is the total number of identified control discontinuities. Bounds on the discontinuity locations are now defined. Assuming that a discontinuity is present somewhere on the mesh interval $\tau \in [\tau_j^{(k)}, \tau_{j+1}^{(k)}]$, to account for the uncertainty incurred by using the numerical solution as a sample for the jump function approximation, a safety factor, $\mu \geq 1$ is introduced to extend the bounds estimated for the discontinuity. This safety factor provides a larger threshold to adequately capture the potential search space of the estimated switch times. Let $[b_i^-, b_i^+]$, $i = \{1, \ldots, n_d\}$ be the lower and upper bounds on the locations of discontinuities in the control (that is, any discontinuity is bounded to lie on the interval $[b_i^-, b_i^+]$). The estimates of these bounds are defined as

$$\left.\begin{aligned} b_i^- &= \tau_{j+\frac{1}{2}}^{(k)} - \mu\left(\tau_{j+\frac{1}{2}}^{(k)} - \tau_j^{(k)}\right), \\ b_i^+ &= \tau_{j+\frac{1}{2}}^{(k)} + \mu\left(\tau_{j+1}^{(k)} - \tau_{j+\frac{1}{2}}^{(k)}\right), \end{aligned}\right\} \quad \begin{aligned} i &= \{1, \ldots, n_d\}, \\ j &= \{1, \ldots, N_k\}, \\ k &= \{1, \ldots, K\}, \end{aligned} \tag{33}$$

where $\tau_{j+\frac{1}{2}}^{(k)} = \frac{1}{2}(\tau_j^{(k)} + \tau_{j+1}^{(k)})$, $j = \{1, \ldots, N_k\}$, $k = \{1, \ldots, K\}$. Larger values of μ are more desirable as it is more likely that the discontinuity b_i will lie in the interval $[b_i^-, b_i^+]$, $i = \{1, \ldots, n_d\}$.

5.2 Identification of Bang-Bang and Singular Domains

Identification of the domains is employed to determine the structure of the control using the discontinuities identified from the jump function approximations. Specifically, the control solution is inspected to determine if any bang-bang or singular arcs exist. The first and second derivatives of the Hamiltonian are computed with respect to the control and analyzed to detect if the Hamiltonian is linear in the control by assessing if the second derivatives are zero. If the Hamiltonian is affine in control, the first derivatives are computed and represent the switching function of the system. If the Hamiltonian is not linear in the control the structure identification process is finished and smooth mesh refinement (see Ref [6]) can be performed.

Suppose the initial solution contains the following newly identified discontinuities b_i and corresponding bounds $[b_i^-, b_i^+]$, $i = \{1, \ldots, n_d\}$. The solution is divided into intervals starting with the initial time, the discontinuity locations, and ending with the final time, $\{[-1, b_1], [b_1, b_i], \ldots, [b_i, b_{i+1}], [b_{i+1}, +1]\}$, $i = \{1, \ldots, n_d\}$. Next, the Hamiltonian in Eq. (13) is computed using the initial solution. The first and second derivatives with respect to the control are computed using the already computed derivatives required by the NLP solver. First, the values of $\mathcal{H}_{uu}$ must be zero. If this condition is satisfied then $\mathcal{H}_u = \phi$ is analyzed as follows. A bang-bang interval in the control structure will occur when the switching function ϕ changes sign. The sign of the switching function ϕ is checked in each interval $[b_i, b_{i+1}]$, $i = \{1, \ldots, n_d\}$. If the sign in the interval is positive, the control is constrained to its minimum value. If the sign in the interval is negative, the control is constrained to its maximum value. A singular interval in the control structure will occur when the switching function ϕ is zero at every point in the interval $[b_i, b_{i+1}]$. If a scenario occurs where the entire control is singular on $[t_0, t_f]$, then no discontinuities will be detected. In this situation, the identification procedure is applied over the entire time domain so that the singular arc can be identified. See Ref. [16] for further details on the identification of bang-bang and singular controls.

5.3 Structure Decomposition

Assuming the methods of Sections 5.1 and 5.2 have identified discontinuities and intervals that are bang-bang or singular, the initial mesh is now decomposed into the multiple-domain structure. Once acquired, the detected structure of the nonsmooth control is used to introduce the appropriate number of domain interface variables, $t_s^{[d]}$, $d = \{1, \ldots, D-1\}$, to be solved for on subsequent mesh iterations, where the initial guess for each variable is the estimated discontinuity location b_i, $i = \{1, \ldots, n_d\}$ that was found using the method in

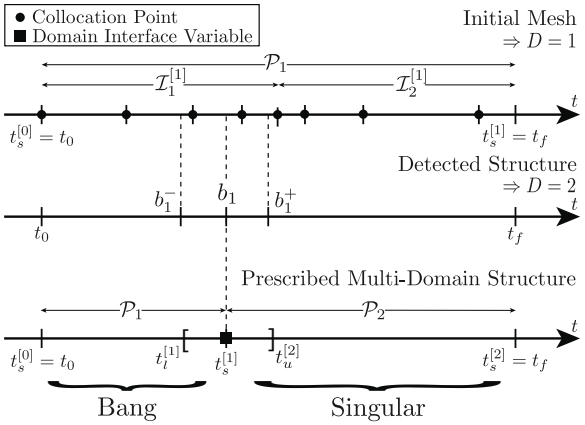

Figure 1: Schematic of the process for decomposing the nonsmooth optimal control problem into D domains where the $D-1$ domain interface variables are included as optimization variables to determine the optimal switch times in the control.

Section 5.1. The domain interface variables are included in the NLP by adding them as additional decision variables that define the new domains, $\mathcal{P}_d = [t_s^{[d-1]}, t_s^{[d]}]$, $d = \{1, \ldots, D\}$. Specifically, the domain interface variables are employed by dividing the time horizon $t \in [t_0, t_f]$ of the original optimal control problem into D domains as described in Section 4.

Next, bounds on the domain interface variables are enforced to prevent the collapse or overlap of domains. The bounds provide an additional constraint on the domain interface variables. The upper and lower bounds on each domain interface variable are determined by taking the discontinuity bounds found in Section 5.1 and transforming them to the time interval $t \in [t_0, t_f]$ using the transformation in Eq. (20). Thus, the bounds $[b_i^-, b_i^+]$, $i = \{1, \ldots, n_d\}$ are transformed to $[t_l^{[d-1]}, t_u^{[d]}]$, $d = \{1, \ldots, D-1\}$.

This approach to structure decomposition partitions the entire problem domain into multiple domains of the form described in Section 4 such that the switch times are represented by the strategically placed domain interface variables $t_s^{[d]}$, $d \in \{1, \ldots, D-1\}$. A schematic for the process of decomposing the nonsmooth control structure into a multiple-domain formulation with domain interface variables is shown in Fig. 1. Additionally, the form of the control in each domain is classified as either bang-bang, singular, or regular. In the next section, the constraints and refinement strategies required by each type of domain are discussed.

5.4 Domain Constraints and Refinement

Once structure identification and decomposition has been performed using the approaches given in Sections 5.1–5.3, additional constraints are required to properly constrain the multiple-domain optimal control problem. Recall that there are three types of domain classifications: bang-bang, singular, and regular. Each domain type requires its own set of constraints and refinement methods. Given that the focus of this paper is on structure identification, the details of these approaches are beyond the scope of this paper and the author refers the reader to Refs. [15] and [16] for further details.

6 Example: Minimum Time Reorientation of a Spacecraft

In this section, a minimum time reorientation of a spacecraft is solved using the structure identification method described in Section 5. The problem contains both finite and infinite-order singular arcs as well as bang-bang arcs across multiple control components. Throughout this section, the structure identification method of this paper is paired with the regularization procedure of [15, 16] and is referred to as the BBSOC method, as in Ref. [16]; however, the results of the structure identification method are exclusively studied in this paper. The results obtained using the method of this paper are compared with a highly accurate numerical solution obtained by enforcing the known structure of the optimal control and also with the optimal control software $\mathbb{GPOPS}-\mathbb{II}$ [30]. The numerical solution obtained by enforcing the known structure of the

optimal control is referred to as a baseline solution. All numerical solutions, other than those obtained using the BBSOC method, are obtained using the MATLAB® optimal control software $\mathbb{GPOPS}-\mathbb{II}$ [30], and $\mathbb{GPOPS}-\mathbb{II}$ is referred to from this point forth as the *hp*-LGR method. For any results obtained where the known structure of the optimal control is not enforced, the problem is formulated as a single-phase optimal control problem for use with the *hp*-LGR method. For any results obtained where the known structure of the optimal control is enforced, the problem is formulated as a multiple-phase optimal control problem for use with the *hp*–LGR method, and the control in each phase is either free (if the control is regular), is set to either its known lower or upper limit (if the control is bang-bang), or is determined by enforcing the singular arc optimality conditions (if the control is sin1gular), and the switch times (which are the endpoints of each phase) are determined as part of the optimization. Finally, for all numerical results obtained, the accuracy of the solution is improved using the mesh refinement method of Ref. [6] where an error analysis is performed using the error estimate described in Ref. [6].

All results are obtained using MATLAB® and the nonlinear program developed in Section 4 is solved using IPOPT [19] in full-Newton mode. The NLP solver tolerance is set to 10^{-8} and the mesh refinement tolerance for smooth mesh refinement [30]) is set to 10^{-6}. All first and second derivatives are supplied to IPOPT using the algorithmic differentiation software ADiGator [31]. The initial mesh consists of ten uniformly spaced mesh intervals and four collocation points per mesh interval, and the initial guess is a straight line for variables with boundary conditions at both endpoints and is a constant for variables with boundary conditions at only one endpoint. Finally, all computations were performed on a 2.9 GHz 6-Core Intel Core i9 MacBook Pro running Mac OS Big Sur Version 11.3 with 32 GB 2400 MHz DDR4 of RAM, using MATLAB® version R2019b (build 9.7.0.1190202).

Consider the following minimum-time rigid body reorientation optimal control problem [32]:

$$\text{minimize} \quad \mathcal{J} = t_f,$$

$$\text{subject to} \quad \left\{ \begin{array}{lcl} \dot{\omega}_1(t) &=& a\omega_{30}\omega_2(t) + u_1(t), \\ \dot{\omega}_2(t) &=& -a\omega_{30}\omega_1(t) + u_2(t), \\ \dot{x}_1(t) &=& \omega_{30}x_2(t) + \omega_2(t)x_1(t)x_2(t) + \frac{\omega_1(t)}{2}(1 + x_1^2(t) - x_2^2(t)), \\ \dot{x}_2(t) &=& \omega_{30}x_1(t) + \omega_1(t)x_1(t)x_2(t) + \frac{\omega_2(t)}{2}(1 + x_2^2(t) - x_1^2(t)), \\ \omega_1(0) &=& \omega_{10}, \quad \omega_1(t_f) = \omega_{1f}, \\ \omega_2(0) &=& \omega_{20}, \quad \omega_2(t_f) = \omega_{2f}, \\ x_1(0) &=& x_{10}, \quad x_1(t_f) = x_{1f}, \\ x_2(0) &=& x_{20}, \quad x_2(t_f) = x_{2f}, \\ |u_i| &\leq& u_{i,\max}, \quad i = 1, 2, \end{array} \right. \tag{34}$$

where $\omega_i(t)$ is the angular velocity, $x_i(t)$ is the position of the spacecraft, ω_{30} is the initial condition for $\omega_3(t)$ which remains constant, and $u_{i,\max} = 1$. For the purposes of demonstrating the capabilities of the structure identification method, two special cases of the optimal control problem given in Eq. (34) will be analyzed. These two cases include a nonspinning axisymmetric rigid body and an inertially symmetric rigid body. It is known for Case 1 that a portion of the optimal solution lies on a second-order singular arc whereas for Case 2 the solution lies on an infinite-order singular arc. For further details of the analysis of the singular controls for these two cases see Ref. [32].

Case 1: Nonspinning Axisymmetric Rigid Body: $(a, \omega_{30}) = (0.5, 0)$

For the case $(a, \omega_{30}) = (0.5, 0)$ and the boundary conditions

$$\begin{array}{rclcrcl} \omega_{10} &=& -0.45 &,& \omega_{1f} &=& 0, \\ \omega_{20} &=& -1.10 &,& \omega_{2f} &=& 0, \\ x_{10} &=& 0.10 &,& x_{1f} &=& 0, \\ x_{20} &=& -0.10 &,& x_{2f} &=& 0, \end{array}$$

a portion of the optimal solution lies on a second-order singular arc [32]. In particular, the control u_1 has a bang-singular structure while the control u_2 is bang-bang (that is, u_2 is not singular). More specifically, the singular optimal control is $u_{1,\text{sing}}^*(t) = 0$ [32]. A baseline solution is obtained using the singular arc condition and known bang-singular structure. The results of the baseline solution are included in Table 1 for comparison.

Table 1: Comparison of computational results for Case 1.

	$t_s^{[1]}$	$t_s^{[2]}$	$t_s^{[3]}$	$t_s^{[4]}$	$t_s^{[5]}$	$\mathcal{J}^*$	δ	ϵ	p
BBSOC	0.6498	1.2898	1.8178	1.9064	1.9919	2.8839	1.24×10^{-10}	10^{-3}	2
hp-LGR	0.6498	1.2897	1.8184	1.9226	1.9922	2.8839	–	–	–
Baseline	0.6498	1.2898	1.8177	1.9054	1.9919	2.8839	–	–	–

The control solutions obtained using the BBSOC and *hp*-LGR methods are shown in Fig. 2 where black solid lines represent the *hp*-LGR solution, red circles represent the BBSOC solution, and blue dashed lines represent the optimal switch times. In particular, Figs. 2a and 2b show that the five switch times are identified using the structure identification method of this paper. Table 1 provides the switch time locations and final time obtained by each of the three methods along with the parameters required for the regularization method. The switch times identified by the structure identification method are also validated by the baseline solution (see Table 1). It is also observed that the switch times obtained by each method seem to be in excellent agreement; however the actual control profiles obtained are not. The control in the last, and singular, domain should be zero, but the solution obtained by the *hp*-LGR method exhibits oscillatory behavior due to the ill-conditioning of the NLP. While the regularization procedure of the BBSOC method is beyond the scope of this paper, the control history of the regularization procedure is provided in Fig. 2e to demonstrate the BBSOC methods ability to remove the oscillations in the singular control.

Figures 2c and 2d show the switching functions that correspond to each of the control components where ϕ_1 and ϕ_2 correspond to u_1 and u_2, respectively. The switching functions are obtained using the initial control solution and are used to identify the switch times and domain types in the control structure. Specifically, the switching functions are used by the structure identification method of this paper to identify the existence of bang-bang arcs and a singular arc.

Finally, Fig. 3a shows the optimal trajectory obtained by the BBSOC method in the $x_1 - x_2$ plane. In the $x_1 - x_2$ plane, if the body is not spinning about its symmetry axis, then an eigenaxis rotation is represented by a straight line. In Fig. 3a, the trajectory along the nonsingular domains do not represent an eigenaxis rotation while the trajectory along the singular domain is an eigenaxis rotation represented by the straight line.

Case 2: Inertially Symmetric Rigid Body: $(a, \omega_{30}) = (0, -0.3)$

For the case $(a, \omega_{30}) = (0, -0.3)$ and the boundary conditions

$$\begin{aligned} \omega_{10} &= 0 \quad , \quad \omega_{1f} = 1, \\ \omega_{20} &= 0 \quad , \quad \omega_{2f} = 2, \\ x_{10} &= 0 \quad , \quad x_{1f} = \text{Free}, \\ x_{20} &= 0 \quad , \quad x_{2f} = \text{Free}, \end{aligned}$$

the optimal solution lies on an infinite-order singular arc [32]. In particular, the control u_1 is totally singular while the control u_2 is bang (that is, u_2 is not singular). More specifically, one possible solution to the singular optimal control is $u^*_{1,\text{sing}}(t) = 0.5$ [32]. The singular arc condition is used to obtain a baseline solution and the results are provided in Table 2 for comparison. The purpose of this maneuver is to accelerate the angular velocity components ω_1 and ω_2 from zero to 1.0 rad/s and 2.0 rad/s, respectively. Thus, the final position is not important in this case leading to x_1 being able to reach its final position in many ways. This causes there to be multiple optimal solutions for the infinite-order singular arc.

For Case 2, the entire control, u_1, lies on a singular arc and the problem does not need to be divided into domains. As a result the structure identification method does not detect any discontinuities and therefore does not assign any domain interface variables. Furthermore, the regularization method of Ref. [15] is applied over the entire time domain. Table 2 provides the optimal objective obtained using the baseline, BBSOC, *hp*-LGR methods. It appears that all three solutions are in agreement; however, it can be seen in Fig. 4a that the control obtained using the *hp*-LGR method is actually incorrect as the solution exhibits highly oscillatory behavior due to the ill-conditioning of the NLP. The second control component in Fig. 4b is bang-bang, but contains no switches so instead it lies at its maximum value.

Figure 3b shows the optimal trajectory in the $x_1 - x_2$ plane where the entire trajectory now lies on a singular arc. However, unlike the results of Case 1, here the singular trajectory is not an eigenaxis rotation

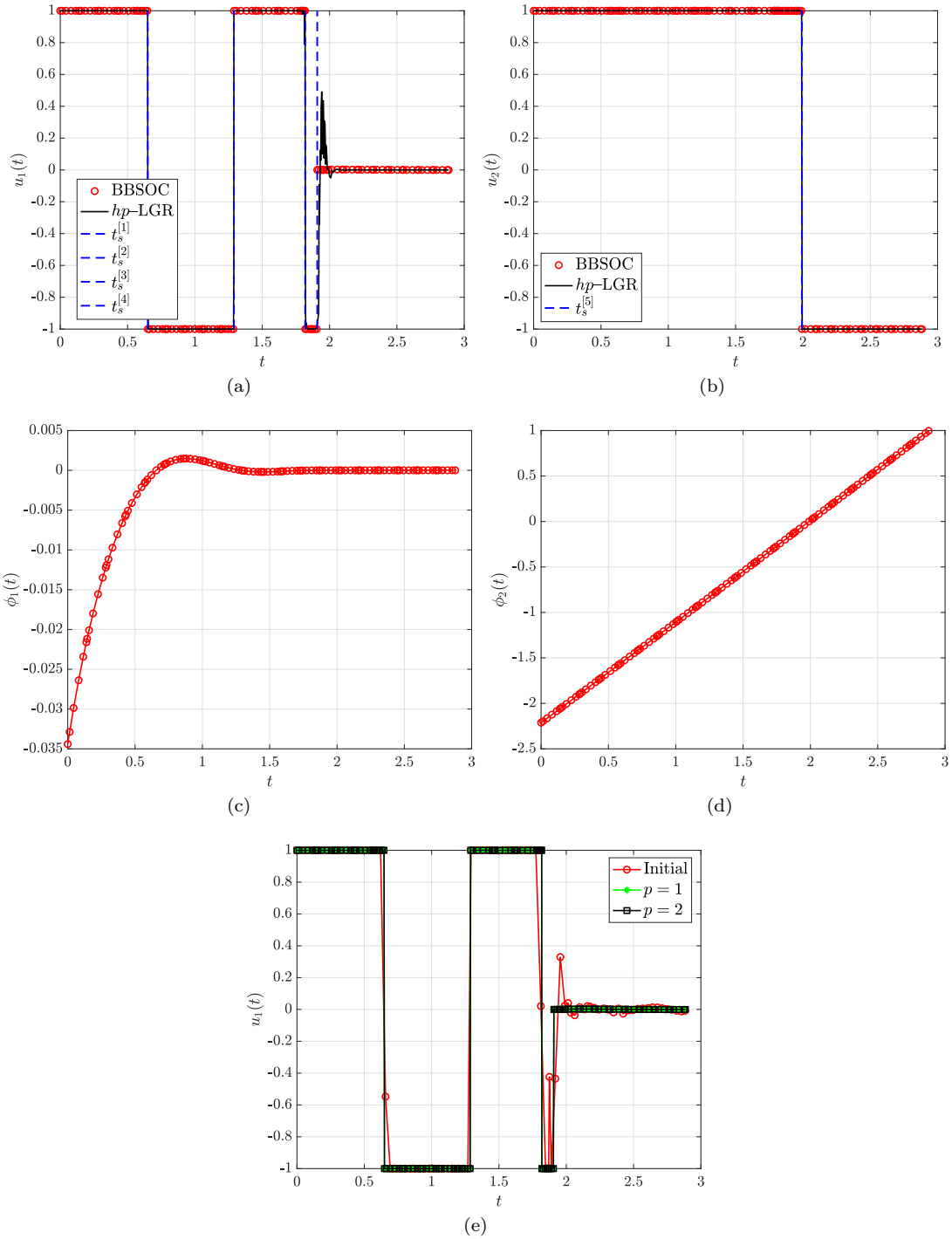

Figure 2: Control component solutions for Case 1 and the corresponding switching function obtained by the BBSOC and *hp*–LGR methods.

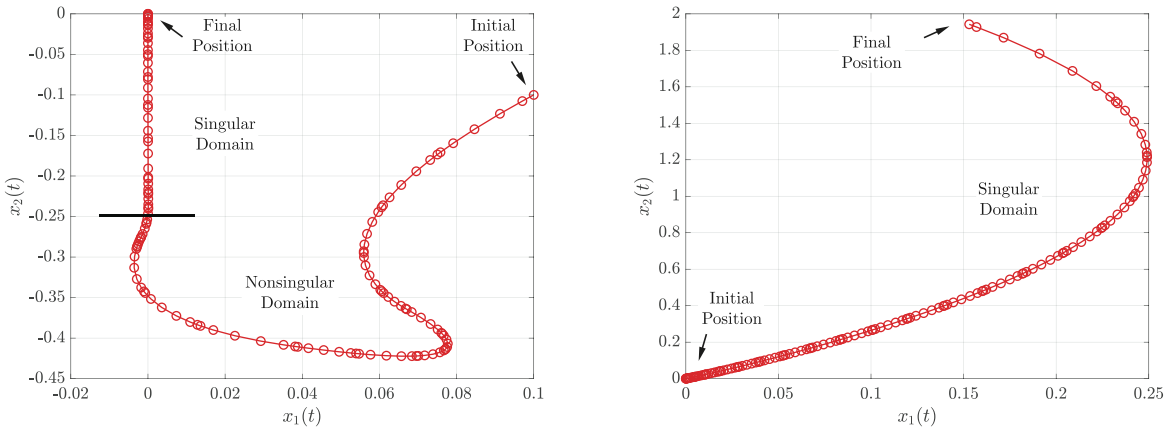

Figure 3: Optimal trajectories for (a) Case 1 and (b) Case 2 in the $x_1 - x_2$ plane.

Table 2: Comparison of computational results for Case 2.

	$\mathcal{J}^*$	δ	ϵ	p
BBSOC	2.00	1.11×10^{-19}	10^{-1}	2
hp-LGR	2.00	–	–	–
Baseline	2.00	–	–	–

due to the nature of the singular arc being of infinite-order. Figure 3b represents one possible trajectory in order to bring the angular velocities to their specified final states as shown in Fig. 4e.

Finally, Fig. 4d shows the switching functions that correspond to each of the control components where ϕ_1 and ϕ_2 correspond to u_1 and u_2, respectively. The switching functions for Case 2 are obtained using the initial control solution and are used to identify that no switch times exist along with the domain types in the control structure. Specifically, the switching functions are used by the structure identification method of this paper to identify the existence of bang-bang arcs and a singular arc.

7 Conclusions

A structure identification method has been described for identifying the structure of nonsmooth and singular optimal control problems using jump function approximations and a multiple-domain formulation of Legendre-Gauss-Radau (LGR) collocation. The structure identification method consists of two stages: identification of the control switch times and domain types and structure decomposition. First, the solution is approximated on an initial mesh. Next, the identification of the switch times in the control and use of the switching function to identify any bang-bang and singular arcs is performed. If the structure detected contains discontinuities and bang-bang and/or singular arcs, the structure is partitioned into a multiple-domain formulation with added decision variables to represent the switch times. Then, the results of the structure identification method can be paired with a strategy for solving bang-bang and singular optimal control problems in order to obtain an accurate numerical solution. The strategy of this method allows for highly accurate approximations of the switch times and nonsmooth control without a priori knowledge of the problem structure. The method has been demonstrated on a complex aerospace problem and it has been shown that the method described in this paper provides accurate solutions to problems whose solutions are either bang-bang or singular when compared against previously developed mesh refinement methods that are not tailored for solving nonsmooth and/or singular optimal control problems.

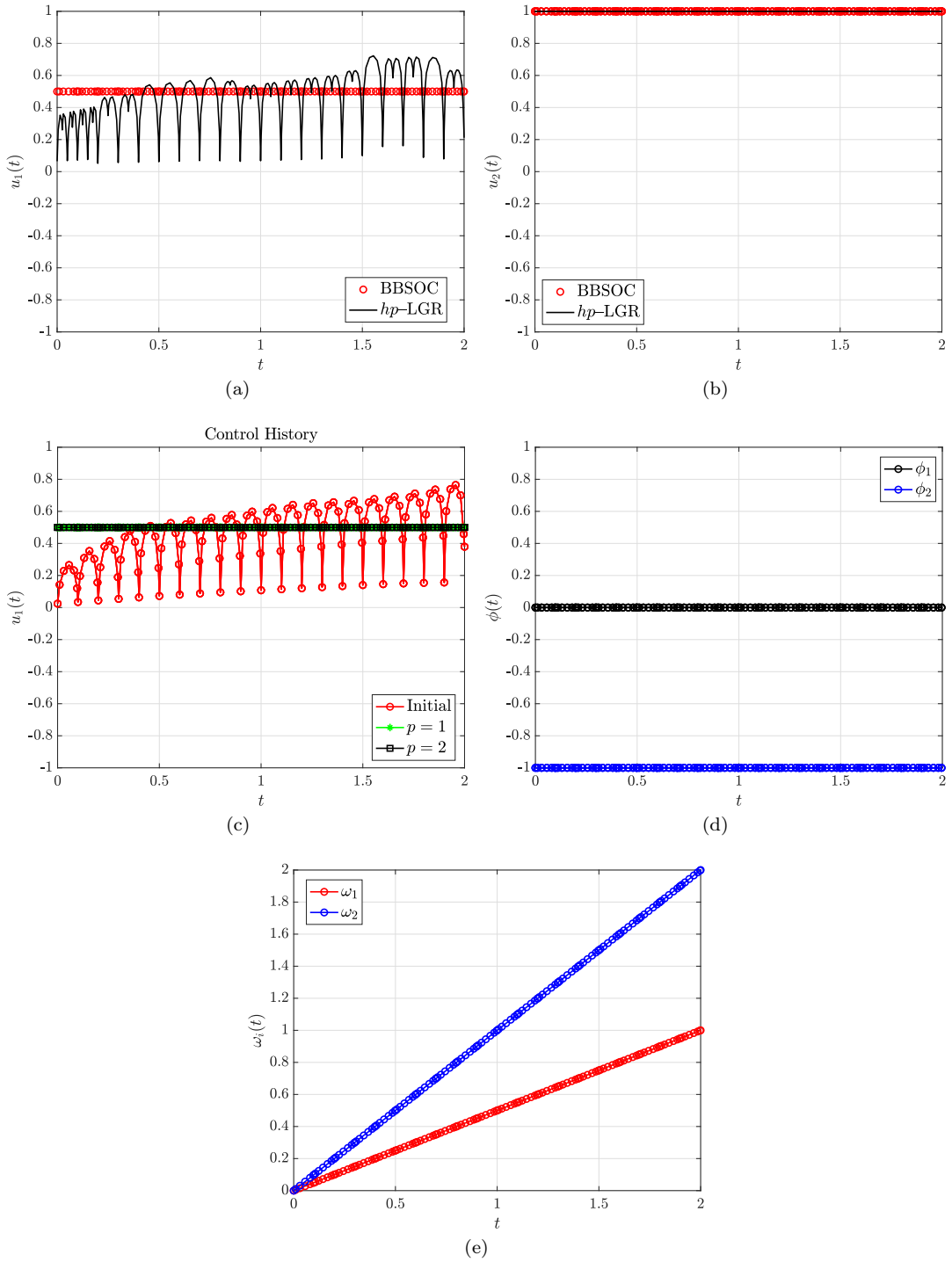

Figure 4: Control component solutions for Case 2 and the corresponding switching function obtained by the BBSOC and *hp*-LGR methods.

8 Acknowledgments

The authors gratefully acknowledge support for this research from the U.S. National Science Foundation under grants DMS-1819002 and CMMI-2031213, the U.S. Office of Naval Research under grant N00014-19-1-2543, and from Lockheed-Martin Corporation under contract 4104177872.

References

[1] Schlegel, M. and Marquardt, W., "Direct Sequential Dynamic Optimization with Automatic Switching Structure Detection," *IFAC Proceedings Volumes*, Vol. 37, No. 9, July 2004, pp. 419–424.

[2] Schlegel, M. and Marquardt, W., "Detection and exploitation of the control switching structure in the solution of dynamic optimization problems," *Journal of Process Control*, Vol. 16, No. 3, March 2006, pp. 275–290.

[3] Wang, P., Yang, C., and Yuan, Z., "The Combination of Adaptive Pseudospectral Method and Structure Detection Procedure for Solving Dynamic Optimization Problems with Discontinuous Control Profiles," *Industrial & Engineering Chemistry Research*, Vol. 53, No. 17, April 2014, pp. 7066–7078.

[4] Chen, W. and Biegler, L. T., "Nested direct transcription optimization for singular optimal control problems," *AIChE Journal*, Vol. 62, No. 10, May 2016, pp. 3611–3627.

[5] Chen, W., Ren, Y., Zhang, G., and Biegler, L. T., "A simultaneous approach for singular optimal control based on partial moving grid," *AIChE Journal*, Vol. 65, No. 6, March 2019, pp. e16584.

[6] Patterson, M. A., Hager, W. W., and Rao, A. V., "A ph mesh refinement method for optimal control," *Optimal Control Applications and Methods*, Vol. 36, No. 4, July–August 2015, pp. 398–421.

[7] Darby, C. L., Hager, W. W., and Rao, A. V., "An hp-adaptive pseudospectral method for solving optimal control problems," *Optimal Control Applications and Methods*, Vol. 32, No. 4, Aug. 2010, pp. 476–502.

[8] Liu, F., Hager, W. W., and Rao, A. V., "Adaptive Mesh Refinement Method for Optimal Control Using Decay Rates of Legendre Polynomial Coefficients," *IEEE Transactions on Control Systems Technology*, Vol. 26, No. 4, July 2018, pp. 1475–1483,.

[9] Agamawi, Y. M., Hager, W. W., and Rao, A. V., "Mesh refinement method for solving bang-bang optimal control problems using direct collocation," *AIAA Scitech 2020 Forum*, 2020, p. 0378.

[10] Aghaee, M. and Hager, W. W., "The Switch Point Algorithm," 2021.

[11] Kaya, C. and Noakes, J., "Computational Method for Time-Optimal Switching Control," *Journal of Optimization Theory and Applications*, Vol. 117, No. 1, April 2003, pp. 69–92.

[12] Mehrpouya, M. A. and Khaksar-e Oshagh, M., "An efficient numerical solution for time switching optimal control problems," *Computational Methods for Differential Equations*, Vol. 9, No. 1, Jan. 2021.

[13] Aronna, M. S., Bonnans, J. F., and Martinon, P., "A Shooting Algorithm for Optimal Control Problems with Singular Arcs," *Journal of Optimization Theory and Applications*, Vol. 158, No. 2, Jan. 2013, pp. 419–459.

[14] Mehra, R. and Davis, R., "A generalized gradient method for optimal control problems with inequality constraints and singular arcs," *IEEE Transactions on Automatic Control*, Vol. 17, No. 1, Feb. 1972, pp. 69–79.

[15] Pager, E. R. and Rao, A. V., "A Method for the Numerical Solution of Singular Optimal Control Problems Using an Adaptive Radau Collocation Method," *AIAA Scitech 2021 Forum*, American Institute of Aeronautics and Astronautics, Jan. 2021.

[16] Pager, E. R. and Rao, A. V., "Method for Solving Bang-Bang and Singular Optimal Control Problems using Adaptive Radau Collocation," *arXiv preprint arXiv:2104.12247*, 2021.

[17] Betts, J. T., *Practical methods for optimal control and estimation using nonlinear programming*, SIAM, 2010.

[18] Gill, P. E., Murray, W., and Saunders, M. A., "SNOPT: An SQP Algorithm for Large-Scale Constrained Optimization," *SIAM Review*, Vol. 47, No. 1, January 2002, pp. 99–131.

[19] Biegler, L. T. and Zavala, V. M., "Large-Scale Nonlinear Programming Using IPOPT: An Integrating Framework for Enterprise-Wide Optimization," *Computers and Chemical Engineering*, Vol. 33, No. 3, March 2008, pp. 575–582.

[20] Benson, D. A., Huntington, G. T., Thorvaldsen, T. P., and Rao, A. V., "Direct Trajectory Optimization and Costate Estimation via an Orthogonal Collocation Method," *Journal of Guidance, Control, and Dynamics*, Vol. 29, No. 6, November-December 2006, pp. 1435–1440.

[21] Garg, D., Patterson, M. A., Hager, W. W., Rao, A. V., Benson, D. A., and Huntington, G. T., "A Unified Framework for the Numerical Solution of Optimal Control Problems Using Pseudospectral Methods," *Automatica*, Vol. 46, No. 11, November 2010, pp. 1843–1851.

[22] Garg, D., Hager, W. W., and Rao, A. V., "Pseudospectral Methods for Solving Infinite-Horizon Optimal Control Problems," *Automatica*, Vol. 47, No. 4, April 2011, pp. 829–837.

[23] Garg, D., Patterson, M. A., Darby, C. L., Francolin, C., Huntington, G. T., Hager, W. W., and Rao, A. V., "Direct Trajectory Optimization and Costate Estimation of Finite-Horizon and Infinite-Horizon Optimal Control Problems via a Radau Pseudospectral Method," *Computational Optimization and Applications*, Vol. 49, No. 2, June 2011, pp. 335–358.

[24] Kameswaran, S. and Biegler, L. T., "Convergence Rates for Direct Transcription of Optimal Control Problems Using Collocation at Radau Points," *Computational Optimization and Applications*, Vol. 41, No. 1, 2008, pp. 81–126.

[25] Miller, A. T., Hager, W. W., and Rao, A. V., "Mesh refinement method for solving optimal control problems with nonsmooth solutions using jump function approximations," *Optimal Control Applications and Methods*, 2021.

[26] Kirk, D. E., *Optimal control theory: an introduction*, Courier Corporation, 2004.

[27] Bryson, A. E. and Ho, Y., *Applied Optimal Control: Optimization, Estimation, and Control*, Hemisphere Publishing Corporation, 1975.

[28] Kelley, H., Kopp, R. E., and Moyer, H. G., "Topics in Optimization, edited by Leitman," 1967.

[29] Kopp, R. E. and Moyer, H. G., "Necessary conditions for singular extremals," *AIAA Journal*, Vol. 3, No. 8, Aug. 1965, pp. 1439–1444.

[30] Patterson, M. A. and Rao, A. V., "GPOPS-II," *ACM Transactions on Mathematical Software*, Vol. 41, No. 1, oct 2014, pp. 1–37.

[31] Weinstein, M. J. and Rao, A. V., "Algorithm 984: ADiGator, a Toolbox for the Algorithmic Differentiation of Mathematical Functions in MATLAB Using Source Transformation via Operator Overloading," *ACM Transactions on Mathematical Software*, Vol. 44, No. 2, Aug. 2017, pp. 1–25.

[32] Shen, H. and Tsiotras, P., "Time-Optimal Control of Axisymmetric Rigid Spacecraft Using Two Controls," *Journal of Guidance, Control, and Dynamics*, Vol. 22, No. 5, Sept. 1999, pp. 682–694.